

## 3-D STUDY OF THE FLAME STABILIZATION ON A TWO-LAYER POROUS BURNER

### Thamy Hayashi

Universidade Federal da Bahia, Department of Chemical Engineering, R. Aristides Novis, 2, 40210-630, Salvador, Brasil  
Currently at Instituto Superior Técnico, Mechanical Engineering Department, Av. Rovisco Pais, 1049-001 Lisboa, Portugal  
thamy@ufba.br

### Isabel Malico

Universidade de Évora, Physics Department, R. Romão Ramalho, 59, 7000-671 Évora, Portugal.  
imbm@uevora.pt

### José Carlos Pereira

Instituto Superior Técnico, Mechanical Engineering Department, Av. Rovisco Pais, 1049-001 Lisboa, Portugal  
jose@navier.ist.utl.pt

**Abstract.** *In this paper, the flame stabilization inside a two-layer radiant burner is numerically studied. The burner is composed by a thin SiC porous foam, which is preceded by a perforated plate made of an insulating material. The model includes the Navier-Stokes, the energy and the chemical species transport equations, and accounts for the local thermal non-equilibrium between the reacting flow and the solid phases and for the radiative heat transfer through the porous matrix. A computer code, based on the aforementioned model and on CFD techniques, and developed to predict detailed thermo-fluid characteristics, has been employed in order to numerically simulate the operational behaviour of porous medium burner device. Predicted temperature, concentration and velocity profiles indicate that the flame front stabilizes inside the ceramic foam for the whole range of operating conditions considered, except for the lower powers and lower excess air coefficient. Furthermore, the model is able to correctly predict the behavior of the burner at the different operating conditions. It is also observed that the jets leaving the perforated plate are strongly dissipated downstream the interface of the two porous layers.*

**Keywords.** *Porous media, combustion, radiation, mathematical modeling, flame stabilization.*

## 1. Introduction

The majority of the household heating burners is based on an open combustion flame, resulting in relatively low thermal efficiency (lower than 30%; Jugjai and Rungsimuntuchart, 2002), low power turndown ratios and considerably big units (Möβbauer *et al.*, 1999). The development of porous burners, where a flame is anchored inside a porous matrix, provides an excellent choice to solve these problems and contributes to considerable energy savings. Also, this kind of burners is associated with low pollutants emissions, namely CO and NO<sub>x</sub> emissions, and with the possibility to burn leaner mixtures and fuels with lower heating values. In 1971, Weinberg proposed several heat recirculating burners, where the flue gas was partially used in the preheating of the reactants. Since then, a lot of effort has been made to demonstrate the practical benefits from heat recirculating burners, especially the porous medium burners (e.g., Hardesty and Weinberg, 1974; Takeno *et al.*, 1981; Echigo *et al.*, 1987; Hsu *et al.*, 1993; Malico *et al.*, 2000; Diamantis *et al.*, 2002).

Numerical modeling plays an important role in the development of porous burners, providing guidance for future designs. In this paper, a numerical study of the flame stabilization in a two-layer radiant burner is presented. The stability ranges of different burners have been determined both experimentally and numerically (e.g., Hsu *et al.*, 1993; Mital *et al.*, 1997; Zhdanok *et al.*, 1998). The burner is composed by a thin SiC porous foam, which is preceded by a perforated plate made of an insulating material.

## 2. Model

The two-layer porous burner prototype modeled in this study was developed at LSTM-Erlangen (Trimis *et al.*, 2001) for household heating and works for 5-20 kW.

The combustion chamber is composed of a thin 10 ppi SiC porous foam, which is preceded by a perforated plate made of an insulating material, Al<sub>2</sub>O<sub>3</sub>. Premixed heptane and air enter the burner through the perforated plate and reaction takes place inside the foam. The flame front is anchored inside the SiC porous matrix, near the interface of the two layers. Fig. (1a) shows a sketch of a sector of the combustion chamber.

### 2.1. Geometric model

In order to perform three-dimensional simulations of combustion inside the burner, a representative unit cell corresponding to a 1/3160 fraction of the volume of the chamber has been considered. A schematic diagram of the

elementary volume considered is shown in Fig. (1b). This procedure allows for the study of the flow at the interface of the two solid layers at a reasonable computational cost.

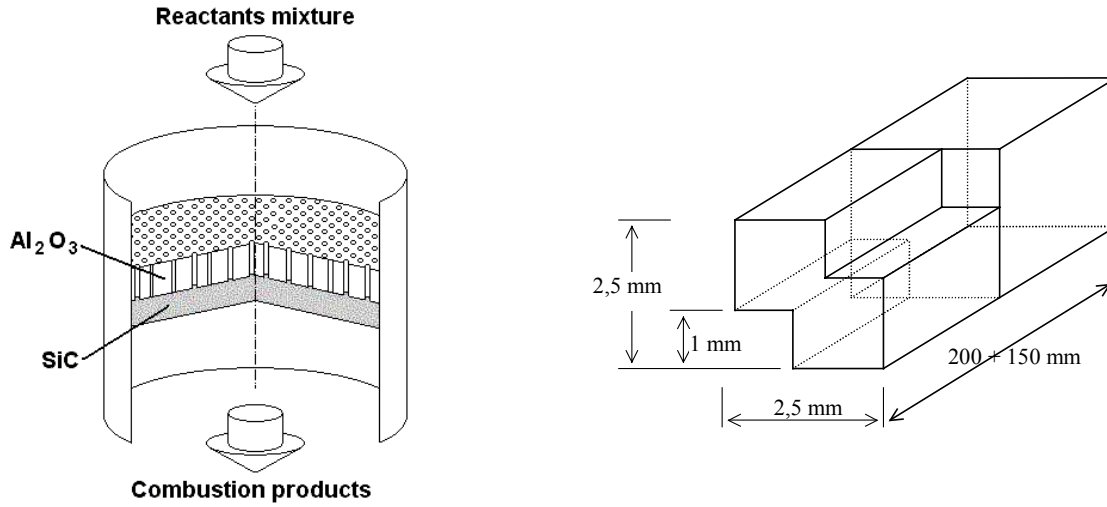


Figure 1. a) Schematic diagram of the combustion chamber; b) Representative unit volume.

## 2.2. Numerical model

Different approaches were used in the modeling of the two porous media. The SiC foam was treated as a single continuum with volume-averaged properties, while direct simulation of the fluid paths was applied for the calculation of the flow in the perforated plate.

Three-dimensional, steady, laminar and Newtonian flow in inert porous media was considered. Local thermal non-equilibrium was assumed, and thus energy balances for both the fluid and the solid phases were performed. Catalytic effects of the high temperature solids were considered negligible. Radiative heat transport was assumed to take place only in the SiC foam, while the gas mixture was considered non radiant. The set of governing equations includes the balances of mass, momentum, energy (for fluid and solid phases) and chemical species, which are written below:

$$\nabla \cdot (\rho \mathbf{v}) = 0 \quad (1)$$

$$\nabla \cdot (\rho \mathbf{v} \otimes \mathbf{v}) = \nabla p + \nabla \cdot (\mu \nabla \mathbf{v}) - (\nabla p)_p \quad (2)$$

$$\nabla \cdot (\rho \mathbf{v} h) - \nabla \cdot \left( \frac{\varepsilon \lambda_f}{c_p} \nabla h \right) = H(T_s - T_f) + \Delta H_c S_{fu} \quad (3)$$

$$0 = \nabla \cdot ((1 - \varepsilon) \lambda_s \nabla T_s) + H(T_f - T_s) - \nabla \cdot \mathbf{q} \quad (4)$$

$$\nabla \cdot (\rho \mathbf{v} Y_i) - \nabla \cdot (\rho D_{im} \nabla Y_i) = -S_{fu} \quad , \quad i \in [1, N_S] \quad (5)$$

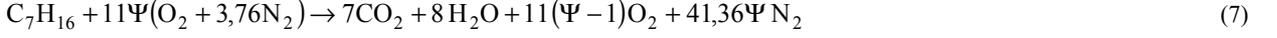
In these equations,  $\rho$  is the density,  $\mathbf{v}$  the velocity vector,  $p$  the pressure and  $\mu$  the viscosity. The gas enthalpy is represented by  $h$ , while  $\varepsilon$  is the porosity of the porous media,  $\lambda_f$  and  $\lambda_s$  the gas and solid thermal conductivity, respectively. Besides that,  $c_p$  is the specific heat of the fluid,  $H$  the volumetric heat transfer between the gas and the solid phases.  $T_s$  and  $T_f$  represent the gas and solid temperatures, while  $\Delta H_c$  is the heat of combustion,  $S_{fu}$  the rate of heptane combustion, and  $\mathbf{q}$  is the radiative flux.  $Y_i$  represents the mass fraction of species  $i$ ,  $N_S$  is the number of chemical species and  $D_{im}$  the diffusion coefficient of the  $i$ -th species in the gas mixture. All thermodynamic and transport properties of the gas-phase are evaluated as functions of temperature, pressure and composition of the mixture by means of specialized code packages (Kee *et al.*, 1995(a), and Kee *et al.*, 1995(b)).

In Eq. (2),  $(\nabla p)_p$  represents the pressure drop due to the porous matrix. This term is set to zero in the perforated plate, and is modeled by the Ergun (1952) model modified by Macdonald *et al.* (1979)

$$\left( \frac{\partial p}{\partial x_i} \right)_p = 180 \frac{(1 - \varepsilon)^2}{\varepsilon^3} \frac{\mu u_i}{d_p^2} + 1,8 \frac{1 - \varepsilon}{\varepsilon^3} \frac{\rho |\mathbf{v}| u_i}{d_p} \quad (6)$$

Since, locally, the solid and gas temperature may be different, separate energy equations for the solid and the gas phases were used. The two equations were coupled through a volumetric convective heat transfer term. This term was set to zero in the perforated plate region, where convection between the gas and the solid phases was treated as a surface convection boundary condition.

The combustion reaction was described by the irreversible one-step reaction.



where  $\Psi$  is the excess air ratio.

The rate of fuel consumption was determined by a one-step Arrhenius rate equation (Kuo, 1986).

$$S_{fu} = A\rho_f^2 Y_{fu} Y_{ox} e^{-E_a/RT} \quad (8)$$

where the pre-exponential factor  $A$  and the activation energy  $E_a$  were taken from Turns (1996) and adapted according to Westbrook *et al.* (1981) and are  $2.88 \times 10^{11} \text{ m}^3 \cdot \text{kmol}^{-1} \cdot \text{s}^{-1}$  and  $1.26 \times 10^5 \text{ kJ} \cdot \text{kmol}^{-1} \cdot \text{K}^{-1}$ , respectively.

Owing to the high emissivity of the solid when compared to the fluid, gas radiation was not considered. To determine the radiative heat flux, the solid and the gas phases were treated as a single continuum homogeneous phase and the radiative transfer equation, Eq. (9), was solved, taking into account emission, absorption and scattering by the porous media.

$$\frac{dI_\eta}{ds} = \hat{s} \cdot \nabla I_\eta = \kappa I_{b\eta} - \beta_\eta I_\eta + \frac{\sigma_{s\eta}}{4\pi} \int_{4\pi} I_\eta(\hat{s}) \Phi_\eta(\hat{s}_i, \hat{s}) d\Omega_i \quad (9)$$

In Eq.(9),  $I$  is the radiative intensity,  $s$  the radiative geometric path length,  $\hat{s}$  the unit vector in a given direction,  $\beta$  the extinction coefficient,  $\sigma$  the scattering coefficient,  $\Phi$  the phase function and  $\Omega$  the solid angle. The subscripts  $\eta$  and  $b$  stand for wavelength and blackbody. The porous medium was assumed to be gray, homogeneous and isotropically scattering.

The boundary conditions that were used are the following:

At the inlet:

$$u=u_{in}; v=0; w=0; T_f=T_{f,in}; Y_i=Y_{i,in} \text{ and } I = \frac{\sigma T_s^4}{\pi} \quad (10)$$

where  $in$  refers to the values at the inlet of the computational domain and  $\sigma$  is the Stephan-Boltzmann constant.

At the outlet:

$$\frac{\partial u}{\partial x} = \frac{\partial v}{\partial x} = \frac{\partial w}{\partial x} = \frac{\partial T_f}{\partial x} = \frac{\partial Y_i}{\partial x} = 0 \text{ and } I = \frac{\sigma T_s^4}{\pi} \quad (11)$$

The temperatures of the solid at the inlet of the perforated plate and at the outlet of the SiC foam were calculated accounting for the radiative heat transfer between the porous matrixes and its surroundings.

$$\lambda_s \frac{\partial T_s}{\partial x} = \sigma(T_{sur}^4 - T_s^4) \quad (12)$$

where  $T_{sur}$  is the temperature of the surroundings.

In the symmetry planes, the normal velocity components were set to zero, as well as the gradients of the other variables.

In the inner surface of the holes, no-slip and impermeability conditions were imposed on the momentum equations and the convective heat transfer between the solid and fluid is accounted for.

### 3. Results

Figure (2a) shows the predicted gas and solid temperature profiles at a hole centerline for a 5 kW power and a 1.8 excess air coefficient, while Fig. (2b) shows, for the some operating conditions, the predicted gas and solid temperature profiles at  $y=z=1.02 \times 10^{-3} \text{ m}$  (in the solid part of the perforated plate).

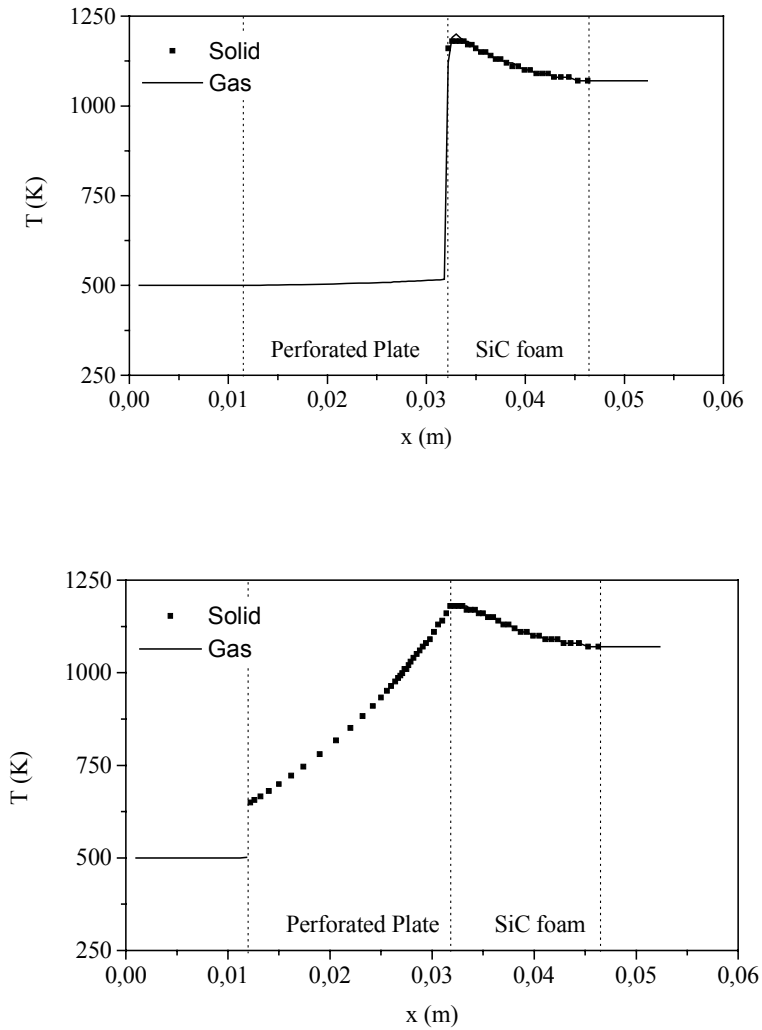


Figure 2. Predicted gas and solid temperature profiles for a 5 kW power and a 1.8 excess air coefficient a) top: at a hole centerline; b) bottom: at  $y=z=1.02 \times 10^{-3}$  m.

Upstream the flame front, the gas temperatures are lower than the solid temperatures, but inside and downstream the flame front the opposite takes place. In the flame front, the chemical energy contained in the gaseous fuel is converted into thermal energy, and the gas temperature is higher than the solid temperature. Due to this temperature difference the porous matrix is heated by convection as the gas flows through the interstices of the porous matrix. Upstream the flame front, the solid phase is heated by conduction and radiation from the reaction zone, and, therefore, the incoming fuel and air mixture is preheated by convection between the hotter solid and the colder gas. It is this preheating of the reactants that is responsible for the good characteristics of porous media combustion. In the perforated plate the temperature differences between the solid and fluid phase is quite big (for the operating conditions of Fig. (2), it reaches more than 650 K). This is due to the relatively low convective heat transfer coefficient of the flow in the perforated plate. If a porous matrix with a higher convective heat transfer coefficient replaced this perforated plate the reactants preheating would be more efficient and the solid and gas temperatures would be similar.

The effect of the operating conditions in the flame characteristics is presented in Fig. (3).

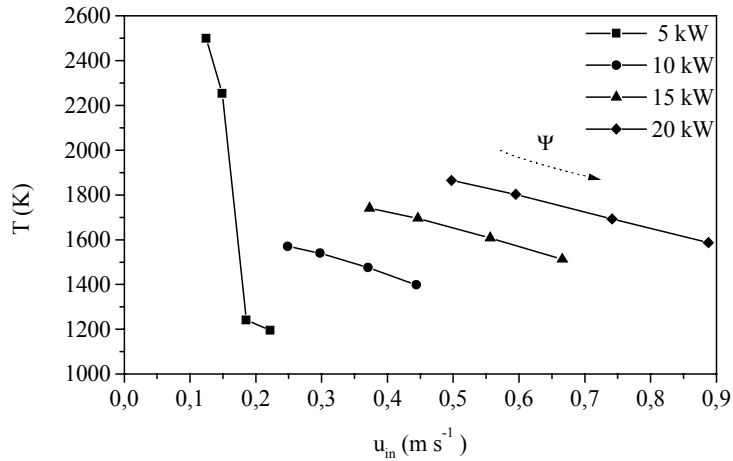


Figure 3. Comparison of the flame temperature for different operating conditions.

When the flame is anchored inside the SiC foam, as the power is increased keeping the excess air ratio constant, the peak temperature gets higher. If, instead, the excess air is increased and the power kept constant, the peak temperature decreases. This behavior is expected.

For the range of operating conditions established for the porous burner studied, the flame front is stabilized at the interface of the perforated plate and the SiC foam, as seen in Fig. (4). The only exceptions occur for the low powers and excess air coefficients. Under these conditions, the flame is stabilized in the holes of the perforated plate, as can be verified, for example, in Fig. (5), that shows the predicted gas and solid temperature profiles at a hole centerline for a 5 kW power and a 1.0 excess air coefficient.

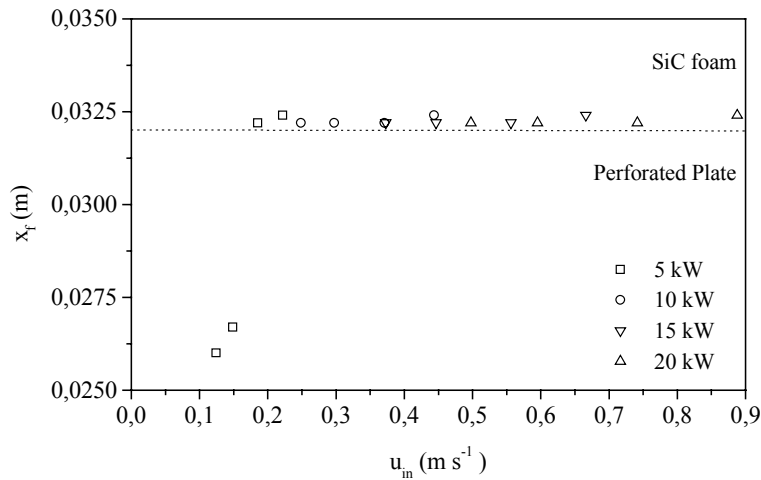


Figure 4. Flame position ( $x_f$ ) for the range of operating conditions modeled.

The stabilization of the flame close to the interface of the solid layers is due to a blockage of the heat diffusion in the solid phase at this position. As was already mentioned, downstream the flame front, the combustion products lose heat to the porous material. In the ceramic foam, part of this heat is diffused toward the burner exit by conduction and radiation, while the balance heat flux is diffused in the upstream direction. Owing to the high extinction of radiation and the low heat conductivity of the perforated plate, this heat flux is blocked at the interface, and is transferred to the reactants flow, helping to support the flame front.

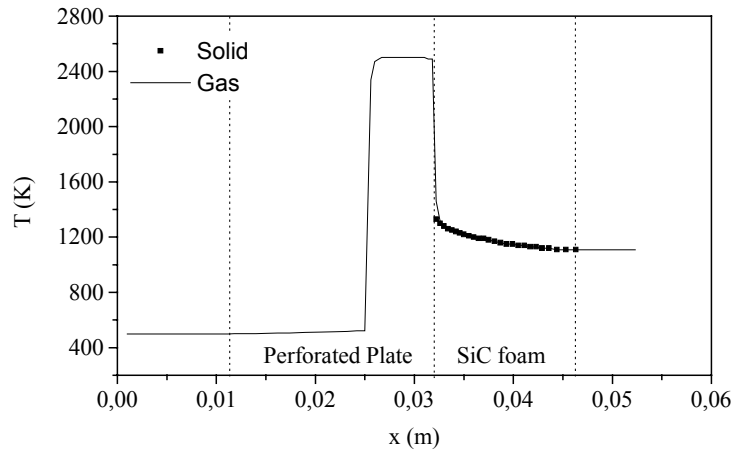


Figure 5. Predicted gas and solid temperature profiles for a 5 kW power and a 1.0 excess air coefficient at a hole centerline.

When the reaction front is placed inside the holes, the flame reaches higher temperatures compared to flames stabilized in the ceramic foam. This is due to the lower energy transfer between solid and fluid in the perforated plate, as discussed above. Since the perforated plate should prevent the occurrence of flashback, these results suggest that the diameter of the holes should be even smaller in burners designed to operate at lower power conditions.

The effect of the ceramic foam on the incoming flow is shown in Fig. (6), which presents iso-surfaces of velocity at the interface of the porous solid layers. Since the characteristic diameter of the void spaces in the SiC foam is larger than the diameter of the holes in the perforated plate, the flow velocity decreases as the fluid enters the second layer.

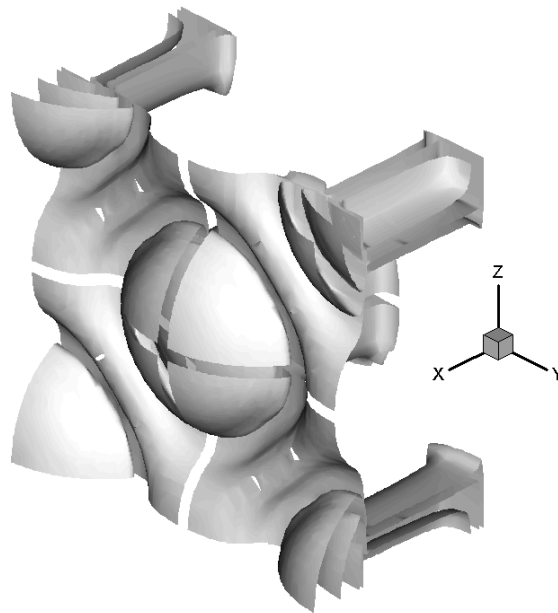


Figure 6. Iso-contours of speed at the interface of the solid layers for power 15 kW and excess air ratio 1.5.

In addition to the deceleration of the flow, there is an intense mixing of the fluid, owing to the presence of the solid struts, and fast dissipation of the jets results. The flow is thus brought toward uniformity after a short distance. This behavior is observed over the whole range of operating conditions studied, as is illustrated in Fig. (7), where contours of the magnitude of the velocity are presented. It is observed that the penetration of the jets in the ceramic foam increases with power and excess air ratio, but that the flow presents fairly uniform speed at the outlet of the thin porous SiC plate.

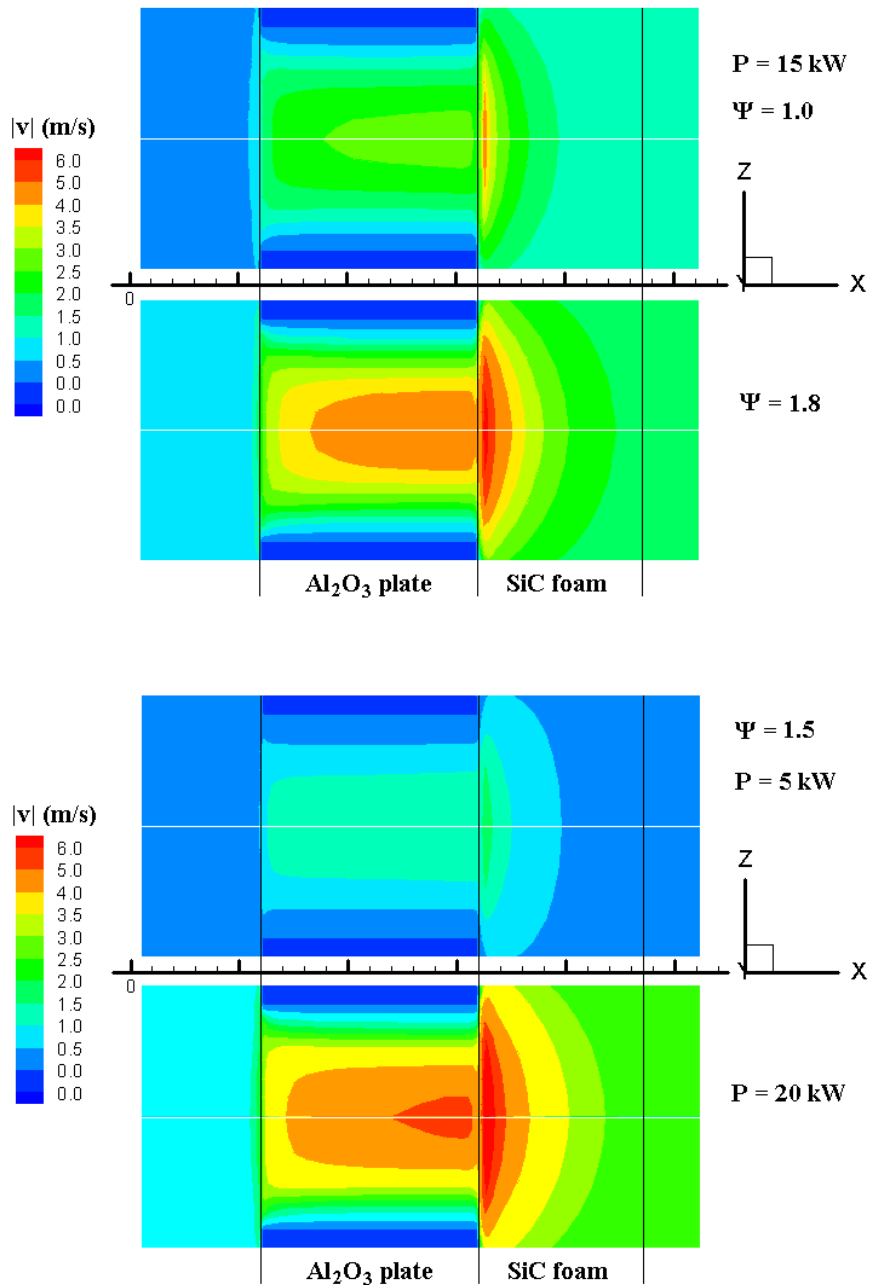


Figure 7. Comparison of jet dissipation behavior for different operating conditions. On top, influence of excess air ratio. In the bottom, the effect of the power.

The effect of the flow mixing within the ceramic foam can also be observed in Fig. (8) and Fig. (9), which show the temperature and the fuel mass fraction profiles, respectively, calculated for operation at a power of 10 kW and 20% excess air.

In both Figs. (8) and (9), the  $xz$ -cuts are made at the lower hole centerline, such as to show the solid and the hole in the perforated plate, while the crossflow  $yz$ -cuts correspond to the first calculation plan downstream the interface of the solid layers, where the distance of grid points in the axial direction is  $4 \times 10^{-4}$  m. The latter show that after flowing for a short distance within the ceramic foam, both the mixture temperature and the fuel concentration present moderately uniform profiles.

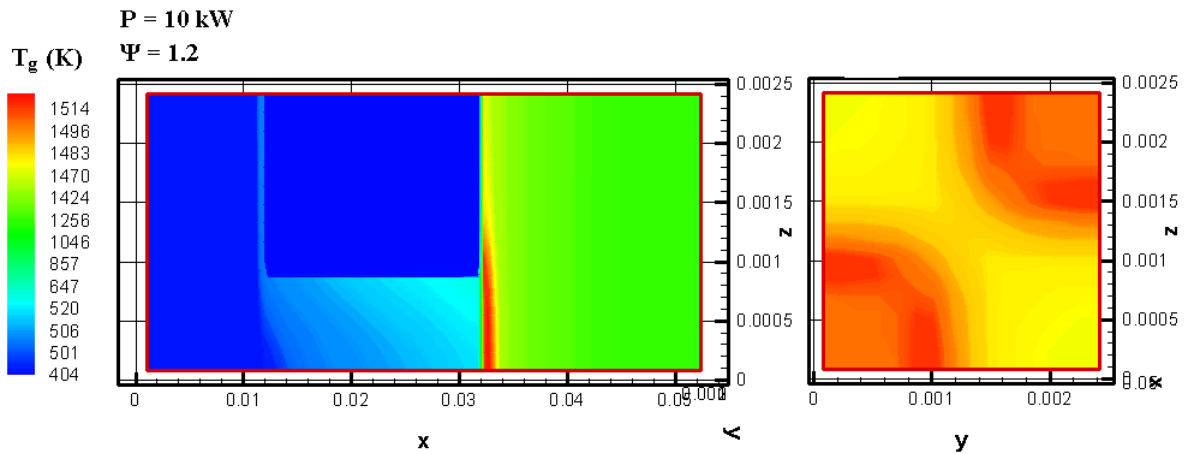


Figure 8. Gas temperature profiles at two sections (on the left side,  $y=0$ ; on the right side,  $x=3.22 \times 10^{-2}$  m), for operation at 10 kW and excess air ratio 1.2.

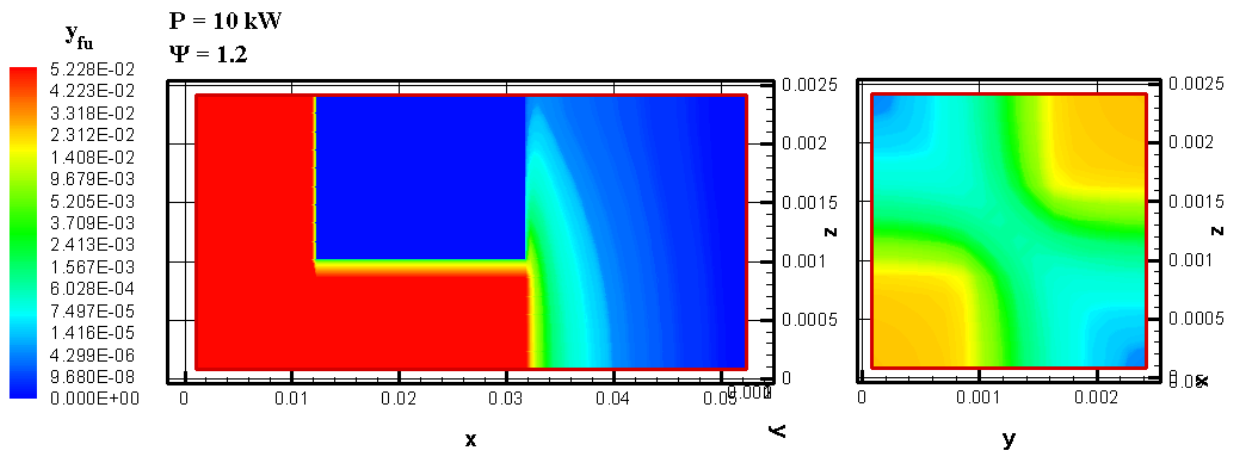


Figure 9. Fuel mass fraction profiles at two sections, for operation at 10 kW and excess air ratio 1.2. (On the left side,  $y=0$ ; on the right side,  $x=3.22 \times 10^{-2}$  m)

In the same fashion, the temperature of the solid is presented in Fig. (10). It is possible to observe that the perforated plate is submitted to an accentuated temperature gradient close to the interface with the ceramic foam. The highest temperatures are observed in the foam, near the interface. For the whole set of operating conditions simulated in this work, the temperature of the solid is not high, which is a desirable characteristic of combustion in two-layer porous burner, as it promotes reduced emission of pollutants and prevents damaging of the materials (Diamantis *et al.*, 2002).

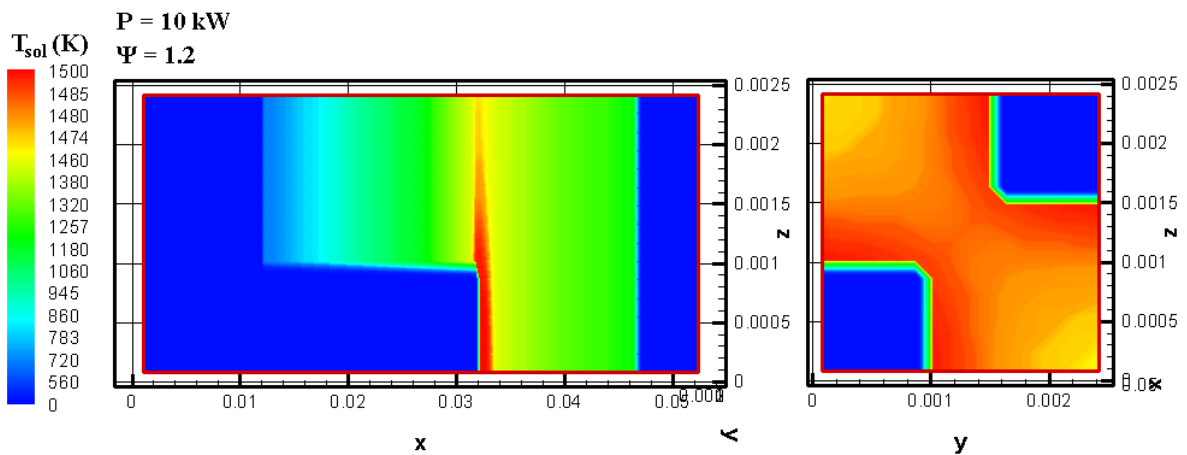


Figure 10. Solid temperature profiles at two sections (on the left side,  $y=0$ ; on the right side,  $x=3.18 \times 10^{-2}$  m), for operation at 10 kW and excess air ratio 1.2.

#### 4. Conclusions

A numerical study of a two-layer porous burner is presented. For a representative element corresponding to 1/3160 of the volume of the burner, the three-dimensional Navier-Stokes equations were solved, along with the equations of continuity, energy balances for both the solid and the fluid phases and transport of chemical species. The model, which accounted for radiative heat transport in the solid, convective heat exchange between solid and fluid and detailed calculation of thermodynamic and transport properties, was solved by means of CFD techniques. One-step global oxidation of heptane was considered to model the combustion process.

The burner modeled in this work is designed to operate in the range of 5 to 20 kW with excess air ratio ranging from 1 to 1.8. Simulations were carried out for a large set of operating conditions within these limits.

The main results show that, for the most of the operating conditions considered, the flame front stabilizes in the ceramic foam, near the interface of the two porous layers, except for the low power and low excess air ratio conditions, for which the flame stabilizes inside the holes, close to the exit plane of the perforated plate. This behavior is expected and is due to the blockage of heat transferred in the solid in the counter-flow direction at the interface's position. Owing to the high extinction of radiation and the low conductivity of the material of the perforated plate, an accentuated temperature gradient is observed along this layer. Nevertheless, the temperature of the solid materials is not high, which is desirable to prevent damaging of the porous layers. It is also observed that the intense mixing of the flow within the interstices of the ceramic foam promotes strong dissipation of the jets produced at the outlet plane of the perforated plate, resulting in fairly planar speed profiles after a short distance within the large-pores SiC layer.

#### 5. Acknowledgement

The first author would like to thank the Fundação CAPES (Brasília, Brazil) for the PhD fellowship granted.

#### 6. References

- Diamantis, D. J., Mastorakos, E. and Goussis, D. A., 2002, "Simulations of Premixed Combustion in Porous Media", *Combustion Theory Modelling*, Vol. 6, pp. 383-411.
- Echigo, R., Kurusu, M., Ichimiya, K. and Yoshizawa, Y., 1987, "Combustion Augmentation of Extremely Low Calorific Gases (Application of the Effective Energy Conversion Method from Gas enthalpy to Thermal Radiation)", *Proceedings of the ASME/JSME Thermal Engineering Joint Conference*, Vol.4, Honolulu, USA, pp. 99-103.
- Ergun, S., 1952, "Fluid Flow through Packed Columns", *Chemical Engineering Progress*, Vol. 48, pp. 89-94.
- Hardesty, D. R. and Weinberg, F. J., 1974, "Burners Producing Large Excess Enthalpies", *Combustion, Science and Technology*, Vol. 8, pp. 201-214.
- Hsu, P.-F., Evans, W. D. and Howell, J. R., 1993, "Experimental and Numerical Study of Premixed Combustion within Nonhomogeneous Porous Ceramics", *Combustion, Science and Technology*, Vol. 90, pp. 149-172.
- Jugjai, S. and Rungsimuntuchart, N., 2002, "High Efficiency Heat-recirculating Domestic Gas Burners", *Experimental Thermal and Fluid Science*, Vol. 26, pp. 581-592.
- Kee, R. J., Rupley, F. M. and Miller, J. A., 1995(a), "Chemkin-II: A Fortran Chemical Kinetics Package for the Analysis of Gas-Phase Chemical Kinetics", Sandia Report SAND89-8009B • UC-706, USA.
- Kee, R. J., Dixon-Lewis, G., Warnatz, J., Coltrin, M. E. and Miller, J. A., 1995(b), "A Fortran Computerr Code Package for the Evaluation of Gas-Phase Multicomponent Transport Properties", Sandia Report SAND86-8246 • UC-401, USA.
- Kuo, K.K., 1986, "Principles of Combustion", John Wiley and Sons, New York, USA, 810p.
- Macdonald, I.F., El-Sayed, M.S., Mow, K. and Dullien, F.A.L., 1979, "Flow through Porous Media – Ergun Equation Revisited," *Ind. Eng. Chem. Fundam.*, Vol. 18, pp. 199-208.
- Malico, I., Zhou, X.-Y. and Pereira, J. C. F., 2000, "Two-dimensional Numerical Study of Combustion and Pollutants Formation in Porous Burners", *Combustion, Science and Technology*, Vol. 152, pp. 57-59.
- Mital, R., Gore, J. P. and Viskanta, R., 1997, "A Study of the Structure of Submerged Reaction Zones in Porous Ceramic Radiant Burners", *Combustion and Flame*, Vol. 111, pp. 3-21.
- Mößbauer, S., Pickenäcker, O., Pickenäcker, K. and Trimis, D., 1999, "Application of the Porous Burner Technology in Energy- and Heat- Engineering", *Proceedings of the 5<sup>th</sup> International Conference on Technologies and Combustion for a Clean Environment*, Vol.1, Lisbon, Portugal, pp. 519-523.
- Takeno, T., Sato, K. and Hase, K., 1981, "A Theoretical Study on an Excess Enthalpy Flame", *Proceedings of the 18<sup>th</sup> Symposium (International) on Combustion*, Waterloo, Canada, pp. 465-472.
- Trimis, D., Wawrzinek, K., Hatzfeld, O., Lucka, K., Rutsche, A., Haase, F., Krüger, K., Küchen, C., 2001, "High Modulation Burner for Liquid Fuels Based on Porous Media Combustion and Cool Flame Vaporization", *Proceedings of the 6<sup>th</sup> International Conference on Technologies and Combustion for a Clean Environment*, Porto, Portugal, pp. 717-724.
- Turns, S. R., 1996, "An Introduction to Combustion: Concepts and Applications", McGraw-Hill, New York, USA, 565 p.
- Weinberg, F. J., 1971, "Combustion Temperatures: the Future?", *Nature*, Vol. 233, pp. 239-241.

- Westbrook, C., and Dryer, F.L., 1981, "Simplified Reaction Mechanisms for the Oxidation of Hydrocarbon Fuels in Flames", *Combustion, Science and Technology*, Vol. 27, pp. 31-43.
- Zhdanok, S. A., Dobrego, K. V. and Futko, S. I., 1998, "Flame Localization inside Axis-symmetric Cylindrical and Spherical Porous Media Burners", *International Journal of Heat and Mass Transfer*, Vol. 41, pp. 3647-3655.